Lawrence Berkeley National Laboratory

Title
Thermal neutron radiative cross sections for Li6,7,Be9,B10,11,C12,13, and N14,15

Authors
Firestone, RB
Revay, Zs

Thermal neutron radiative cross sections for ^{6,7}Li, ^{9}Be, ^{10,11}B, ^{12,13}C, and ^{14,15}N

R. B. Firestone[1] and Zs. Revay[2,3]

[1]*Department of Nuclear Engineering, University of California at Berkeley, Berkeley, California 94720, USA*

[2]*Nuclear Analysis and Radiography Department, Center for Energy Research, Hungarian Academy of Sciences, P.O. Box 49, Budapest 1525, Hungary*

[3]*Heinz Maier-Leibnitz Zentrum (MLZ), Technische Universität München, 85747 Garching, Germany*

Total thermal radiative neutron cross sections have been measured on natural and enriched isotopic targets containing ^{6,7}Li, ^{9}Be, ^{10,11}B, ^{12,13}C, and ^{14,15}N with neutron beams from the Budapest Reactor. Complete neutron capture γ-ray decay schemes were measured for each isotope. Absolute transition probabilities have been determined by a least-squares fit of the transition intensities, corrected for internal conversion, to the (n,γ) decay schemes. The γ-ray cross sections were standardized using stoichiometric compounds containing both the isotope of interest and another element whose γ-ray cross sections are well known. Total cross sections σ_0 were then determined for each isotope from the γ-ray cross sections and transition probabilities. For the ^{11}B$(n,\gamma)^{12}$B reaction decay transition probabilities were determined for the γ rays from ^{12}B ($t_{1/2} = 20.20$ ms) β^- decay.

I. INTRODUCTION

Precise thermal neutron capture γ-ray cross sections have been measured for all naturally abundant elements except He and Pm at the Budapest Reactor [1,2]. These data were evaluated, together with additional information from the literature, to generate the Evaluated γ-ray Activation File (EGAF) [3] and were published in the *Handbook of Prompt Gamma Activation Analysis* [4]. The (n,γ) data can be used to determine total radiative thermal neutron capture cross sections σ_0 if the level scheme is complete as is the case for the light isotopes.

The elements H, Li, Be, and B are important strategic materials identified by the U.S. Department of Defense [5], while the elements C, N, and O are abundant in nature and important for dosimetry, neutron transport calculations, and shielding determinations. Previously we have published the total radiative thermal neutron capture cross sections for ^{2}H and ^{16,17,18}O [6] and in this work we discuss our measurements of the ^{6,7}Li, ^{9}Be, ^{10,11}B, ^{12,13}C, and ^{14,15}N cross sections.

II. EXPERIMENT

The ^{6,7}Li, ^{9}Be, ^{10,11}B, ^{13,14}C, and ^{14,15}N(n,γ) neutron capture γ-ray spectra were measured in both guided thermal and cold neutron beams at the 10-MW Budapest Reactor [1]. Neutrons entered the evacuated target holder and continued to the beam stop at the rear wall of the guide hall. The target station, where both primary and secondary γ rays can be measured in low background conditions, is located $\approx$30 m from the reactor. The neutron flux at the target ranged from 2.3×10^{8} cm^{-2} s^{-1} for cold beams to 5×10^{7} cm^{-2} s^{-1} for thermal beams during these experiments.

Prompt γ rays from the target were measured with an n-type high-purity, 27% efficient, germanium (HPGe) detector with closed-end coaxial geometry located 23.5 cm from the target. The detector is Compton suppressed by a BGO-scintillator guard detector annulus and surrounded by 10-cm-thick lead shielding. Counting efficiency was calibrated from 50 keV to 10 MeV with radioactive sources and (n,γ) reaction γ rays to an accuracy of better than 1% from 0.5 to 6 MeV and better than 3% at other energies [7]. The γ-ray spectra were analyzed with the Hypermet-PC program [7,8].

III. NEUTRON SEPARATION ENERGIES

The γ-ray energy calibrations were also performed using the efficiency calibration sources. Level energies, including the neutron separation energy, were calculated by a least-squares fit of the γ rays to the level scheme with the computer code GAMUT [9]. The χ^2/f quality of each fit of the γ rays to the level scheme is reported in the decays scheme figure captions. Our measured neutron separation energies are compared to the recent compilation of Wang *et al.* [10].

IV. CROSS SECTION ANALYSIS

Natural and isotopically enriched targets were suspended in teflon holders to reduce the target background and irradiated in the neutron beam to obtain high statistics γ-ray spectra. The small contribution from internal conversion for these low-Z isotopes was dominated by internal pair conversion (IPC), which can exceed 0.3% for high energy transitions, and was calculated using the BRICC code [14] assuming multipolarities taken from the Evaluated Nuclear Structure Data File (ENSDF) [15]. This correction had been ignored in earlier work but became more significant in our high precision measurements.

Complete neutron capture decay schemes were constructed for each of the isotopes discussed here. The absolute γ-ray transition probabilities were then determined by a least-squares fit of the transition intensities to the decay scheme where we assume that the intensity is balanced feeding/deexciting each intermediary level and the total primary transition intensity deexciting the capture state (CS) equals the secondary intensity populating the ground state (GS). The

TABLE I. ^{14}N(n,γ) energies, intensities, transition probabilities, and γ-ray cross sections measured on a deuterated urea target enriched to 98% in deuterium.

$E_\gamma(\Delta E_\gamma)$	Mult[a]	MR	ICC(ΔICC)	$I_\gamma(\Delta I_\gamma)$	$P_\gamma(\Delta P_\gamma)$	$\sigma_\gamma(\Delta\sigma_\gamma)$[b]	$\sigma_0(\Delta\sigma_0)$
131.44(7)[c]	E1		0.00053(1)	0.062(12)	0.019(3)		
383.0(4)[c]	E1		$1.86(3)\times10^{-5}$	0.025(8)	0.0076(16)		
583.57(3)	M1		$7.30(11)\times10^{-6}$	0.62(21)	0.138(23)		
609.19(13)	M1		$6.70(10)\times10^{-6}$	0.23(3)	0.075(6)		
767.67(12)	M1		$4.27(6)\times10^{-6}$	0.24(3)	0.068(6)		
770.4(5)[c]	E1		$3.12(5)\times10^{-6}$	0.033(12)	0.010(4)		
831.39(14)	E1		$2.64(4)\times10^{-6}$	0.16(3)	0.048(9)		
908.41(7)	E1		$2.20(3)\times10^{-6}$	0.59(4)	0.178(11)		
977.1(3)	E1		$1.90(3)\times10^{-6}$	0.12(4)	0033(12)		
1 011.61(8)	M1		$2.56(4)\times10^{-6}$	0.6(4)	0.10(7)		
1 025.2(3)[c]	E1		$1.73(25)\times10^{-6}$	0.054(8)	0.0163(24)		
1 053.9(3)[c]	E1		$1.64(23)\times10^{-6}$	0.050(12)	0.015(4)		
1 073.04(13)	E1		$1.59(2)\times10^{-6}$	0.27(3)	0.079(6)		
1 157.52(4)[c]	E2		$7.27(11)\times10^{-6}$	0.21(10)	0.05(3)		
1 297.7(3)[c]	M1+E2	0.32^{+10}_{-9}	$2.18(7)\times10^{-5}$	0.0012(5)	0.00036(15)		
1 416.28(12)[c]	M1		$4.29(6)\times10^{-5}$	0.026(4)	0.0079(12)		
1 479.7(9)[c]	M1+E2	0.149^{+5}_{-6}	$5.84(9)\times10^{-5}$	0.00092(7)	0.000278(21)		
1 549.9(3)[c]	M1+E2	0.11(3)	$7.88(12)\times10^{-5}$	0.00013(7)	0.000039(21)		
1 610.79(14)[c]	E1		0.00036(1)	0.246(21)	0.075(6)		
1 612.13(18)	E1		0.00036(1)	0.12(5)	0.038(13)		
1 652.1(3)[c]	E1		0.00039(1)	0.00013(7)	0.000039(21)		
1 678.24(3)	M1		$1.20(2)\times10^{-4}$	26.05(17)	7.81(5)	6.26(4)	80.2(7)
1 681.17(4)	E1		0.00041(1)	5.33(4)	1.609(12)		
1 748.77(7)[c]	M1		$1.45(2)\times10^{-4}$	0.009(3)	0.0027(9)		
1 783.54(7)	M1		$1.58(2)\times10^{-4}$	0.77(5)	0.232(14)		
1 853.94(5)	M1		$1.85(3)\times10^{-4}$	1.97(9)	0.63(3)		
1 878.2(3)[c]	E1		0.00056(1)	0.0009(4)	0.00027(12)		
1 884.85(3)	M1+E2	0.014^{+15}_{-1}	$1.97(3)\times10^{-4}$	60.6(4)	18.32(8)	14.57(9)	79.5(7)
1 921.2(8)[c]	E1		0.00059(1)	0.0067(21)	0.0020(6)		
1 988.53(8)	M1		0.00024(1)	1.22(7)	0.361(21)		
1 999.69(3)	M1		$2.42(4)\times10^{-4}$	13.11(8)	3.976(23)	3.15(2)	79.2(7)
2 002.3(4)[c]	M1+E2	0.31(15)	0.00025(1)	0.79(17)	0.18(5)		
2 030.86(24)	M1+E2	0.18(15)	0.00026(1)	0.25(4)	0.073(12)		
2 247.44(12)[c]	E1		0.00081(1)	0.010(5)	0.0031(15)		
2 262.02(17)	M1		0.00035(1)	0.21(3)	0.063(9)		
2 293.15(16)[c]	M1+E2	0.028(12)	0.00036(1)	0.150(17)	0.048(5)		
2 389.1(3)[c]	E1		0.00090(1)	0.00050(21)	0.00015(6)		
2 520.45(4)	M1		0.00046(1)	17.85(17)	5.42(5)	4.29(4)	79.2(9)
2 604.8(10)[c]	E1		0.00104(2)	0.0054(12)	0.0016(4)		
2 726.0(5)[c]	E1		0.00110(2)	0.067(17)	0.020(5)		
2 830.80(5)	E1		0.00116(2)	5.53(17)	1.74(4)		
2 898.4(5)[c]	M1		0.00061(1)	0.075(17)	0.022(5)		
3 013.63(6)	M1		0.00066(1)	2.67(10)	0.79(3)		
3 269.2(4)[c]	E2		0.00090(1)	0.20(4)	0.048(5)		
3 294.3(3)[c]	E1+M2	0.13^{+3}_{-4}	0.00137(2)	0.0013(5)	0.00039(15)		
3 300.92(24)	M1+E2	0.91(7)	0.00083(1)	0.37(5)	0.117(15)		
3 400.7(3)[c]	E1		0.00143(2)	0.0015(8)	0.00045(24)		
3 435.8(10)[c]	M1		0.00082(1)	0.0083(21)	0.0025(6)		
3 531.98(5)	M1		0.00086(1)	29.67(25)	9.05(7)	7.13(6)	78.8(8)
3 546.4(3)[c]	E1		0.00150(2)	0.00025(12)	0.00008(4)		
3 677.80(5)	M1		0.00091(1)	47.7(4)	14.39(9)	11.47(10)	79.7(8)
3 779.04(7)[c]	E2		0.00110(2)	0.071(21)	0.022(6)		
3 855.55(8)	E2		0.00112(2)	2.52(10)	0.78(3)		
3 881.4(5)	E1		0.00163(2)	0.27(6)	0.095(17)		
3 884.35(11)	M1		0.00098(1)	1.76(8)	0.545(24)		
3 923.9(6)[c]	E1		0.00165(2)	0.12(3)	0.034(7)		

TABLE I. (*Continued*).

$E_\gamma(\Delta E_\gamma)$	Mult[a]	MR	ICC(ΔICC)	$I_\gamma(\Delta I_\gamma)$	$P_\gamma(\Delta P_\gamma)$	$\sigma_\gamma(\Delta\sigma_\gamma)$[b]	$\sigma_0(\Delta\sigma_0)$
4 125.3(3)[c]	M1+E2	0.59(13)	0.00110(2)	0.008(3)	0.0024(9)		
4 377.4(3)[c]	M1+E2	0.135(15)	0.00114(2)	0.0025(12)	0.0008(4)		
4 508.69(6)	E1		0.00186(3)	55.3(5)	16.62(11)	13.28(11)	79.9(8)
4 654.1(11)[c]	E1		0.00191(3)	0.096(21)	0.029(6)		
4 795(1)[c]	M1		0.00126(2)	0.0079(17)	0.0024(5)		
5 178.5(3)[c]	E1		0.00208(3)	0.014(6)	0.0042(15)		
5 268.98(7)	M2+E3	0.131(13)	0.00112(2)	100.0(9)	30.17(14)	24.03(21)	79.6(8)
5 297.66(15)	E1		0.00211(3)	71.1(8)	21.65(14)	17.08(19)	78.9(10)
5 402.1(3)[c]	E1+M2	0.13^{+7}_{-8}	0.00212(4)	0.00050(21)	0.00015(6)		
5 430.6(3)[c]	E1+M2	0.24^{+4}_{-8}	0.00209(5)	0.025(12)	0.007(3)		
5 533.25(8)	M1		0.00146(2)	65.8(6)	19.86(14)	15.82(15)	79.7(9)
5 561.95(8)	M1		0.00147(2)	36.1(4)	10.90(11)	8.67(9)	79.5(9)
6 322.30(9)	M1+E2	0.132(4)	0.00165(2)	62.0(5)	18.82(11)	14.89(13)	79.1(8)
7 153.4(4)[c]	E3		0.00171(2)	0.212(25)	0.064(8)		
7 298.90(10)	E1+M2	0.017^{+3}_{-8}	0.00067(1)	32.0(3)	9.50(8)	7.68(8)	80.8(10)
8 310.17(13)	E1		0.00278(4)	13.90(21)	4.15(6)	3.34(5)	80.5(13)
8 568.9(7)	E1+M2	0.85^{+3}_{-9}	0.00216(4)	0.22(6)	0.073(17)		
9 047.3(4)	E1		0.00290(4)	0.61(10)	0.187(15)		
9 149.24(17)	M1		0.00210(4)	4.74(21)	1.586(22)		
9 219.5(11)[c]	M1		0.00211(4)	0.062(25)	0.018(6)		
9 923.4(7)	M1		0.00221(4)	0.34(8)	0.102(16)		
10 061.85(5)	E1		0.00306(4)	0.19(3)	0.066(6)		
10 697.8(17)	M1+E2	0.180^{+2}_{-6}	0.00231(4)	0.033(17)	0.010(4)		
10 829.10(21)	E1		0.00317(4)	44.5(17)	13.44(21)	10.7(4)	79.6(3)
					Weighted average total cross section		80.0(4)

[a]Multipolarity assumed from the level J^π values and used for the calculation of internal conversion coefficients.
[b]Cross sections reported by Belgya [11].
[c]Previously observed transitions from the literature [12,13] that were too weak to observe here.

fitted transition probabilities provide a well balanced, energy conserving decay scheme.

The γ-ray cross sections were standardized using stoichiometric high purity targets containing the isotope of interest and a comparator isotope that emits γ rays with well known cross sections. Each target was analyzed by PGAA to search for γ rays from target impurities and no significant impurities were found for the targets used in these experiments. The primary comparator for this work is the 2223-keV transition produced by the ^{1}H(n,γ) reaction where $\sigma_\gamma = 332.5 \pm 0.7$ mb [6,16]. The secondary standards ^{12}C and ^{14}N were calibrated with respect to hydrogen as discussed below. The total radiative thermal neutron cross sections are calculated as shown in Eq. (1) where Abd(%) is percent abundance of the isotope of interest in the target. This method eliminates

$$\sigma_0 = \frac{\sigma_\gamma}{P_\gamma(\%)\text{Abd}(\%)} \times 10^4, \tag{1}$$

the need to know the absolute neutron flux or the neutron spectrum for these non-1/v isotopes. For natural targets we use the standard abundances of Berglund and Wieser [17] and for enriched targets we use the abundances reported for the material.

Uncertainties in the cross section measurements are derived from the statistical uncertainties in the peak analysis of the γ-ray spectrum, determined by Hypermet, added in quadrature with the systematic uncertainties in the isotopic abundance

and standardization γ-ray cross sections. Each cross section discussed here is the result of several measurements and the goodness of fit for each weighted average value is determined by a χ^2/f test where f is the number of degrees of freedom.

A. ^{14}N cross section

A 98% enriched deuterated urea (CD$_4$N$_2$O) target was irradiated for 233 034 s at the Budapest Reactor. 80 γ rays, including 38 γ rays observed in other experiments [12,13] but too weak to be seen here, were placed in the ^{15}N level scheme and are listed in Table I. The transition probabilities were fit to the capture γ-ray decay scheme, as discussed above, with a $\chi^2/f = 0.42$. The ^{15}N capture γ-ray decay scheme is shown in Fig. 1, where the level energies are calculated by a least-squares fit to the γ-ray energies. The neutron separation energy, determined in this work, is $S_n = 10\,833.22 \pm 0.05$ keV in agreement with the recommended value $S_n = 10\,833.2951 \pm 0.0008$ keV [10].

The 1884.85 keV γ-ray cross section from ^{14}N(n,γ) was standardized with respect to hydrogen using a variety of stoichiometric compounds summarized in Table II yielding a weighted average cross section from the seven measurements of 14.57 ± 0.04 mb. The uncertainty includes a statistical error of 0.02 mb and a calibration error of 0.03 mb. The same calibration cross section was used by Belgya [11] to calibrate the γ-ray cross sections of 14 strong transitions in

FIG. 1. Decay scheme for $^{14}N(n,\gamma)$. Total transition probabilities $P_{\gamma+e}$ are shown. The fit of the γ rays to the level scheme gives $\chi^2/f = 1.3$.

^{15}N ranging from 1.7 to 8.3 MeV shown in Table I. Another accurate set of $^{14}N(n,\gamma)$ cross sections are available from Jurney *et al.* [13], but we chose the Belgya data because it corrects for an earlier systematic uncertainty in the high energy efficiency calibration. We also measured the cross section of the 10829.10 keV CS $\rightarrow$ GS γ ray as 10.7 ± 0.4 mb. The total

radiative cross sections derived from all 15 measurements are consistent and led to a weighted average value of $\sigma_0(^{14}N) = 80.0 \pm 0.4$ mb with a statistical uncertainty of 0.02 mb and a calibration uncertainty of 0.03 mb. This result is consistent with the previous measurements that are summarized in Table III.

TABLE II. Calibration of the 1884.85 keV γ-ray cross section. The ^{14}N natural abundance of $99.632 \pm 0.007\%$ [17] was used for calculating the isotopic cross section. The weighted average includes an 0.02 mb statistical uncertainty with $\chi^2/f = 1.6$ and a calibration uncertainty of 0.03 mb.

Compound	Formula	$\sigma_\gamma(\Delta\sigma_\gamma)$ mb
Pyridine	C_5H_5N	14.66 ± 0.07
Melamine	$C_3H_6N_6$	14.50 ± 0.04
Urea	CH_4N_2O	14.70 ± 0.18
Ammonium sulfate	$(NH_4)_2SO_4$	14.88 ± 0.14
Ammonium nitrate-1	NH_4NO_3	14.65 ± 0.09
Ammonium nitrate-2	NH_4NO_3	14.59 ± 0.17
Ammonium nitrate-3	NH_4NO_3	14.56 ± 0.10
	Weighted average	14.57 ± 0.04

TABLE III. Comparison of the previous measurements of the $^{14}N(n,\gamma)$ cross section. All measurements were done by the PGAA method.

σ_0 (mb)	Reference
160 ± 90	Kinsey (1951) [18]
80 ± 20	Bartholomew (1957) [19]
75.0 ± 7.5	Jurney (1963) [20]
79.7 ± 2.4	Islam (1981) [21]
80.1 ± 2.0	Islam (1990) [22]
80.3 ± 0.6	Jurney (2002) [13]
79.5 ± 1.3	Loginov (2005) [23]
80.3 ± 0.8	Belgya (2006) [11]
80.1 ± 0.6	Mughabghab (2006) [16]
80.0 ± 0.4	This work

TABLE IV. ^{15}N(n,γ) γ-ray energies, transition probabilities, and total cross sections measured on a pyridine target enriched to 98% in ^{15}N. Two independent measurements were made of the 6129 keV γ ray from ^{16}N β^- decay. The uncertainty in the weighted average is nearly entirely statistical with $\chi^2/f = 0.03$.

E_γ	Mult[a]	ICC(ΔICC)	$P_\gamma(\Delta P_\gamma)$	$\sigma_\gamma(\Delta\sigma_\gamma)$	$\sigma_0(\Delta\sigma_0)$
					(μb)
298	M1	$3.02(5)\times10^{-5}$	99.9970(5)	39.9(17)	39.9(17)
2192	E2	$4.09(6)\times10^{-4}$	99.959(6)	37.7(75)	37.7(75)
6129-1	{E3		67.0(6)[b]}	25.9(44)	38.6(66)
6129-2		0.00147(21)		26.4(18)	39.4(27)
			Weighted average		39.6(14)

[a]From Tilley *et al.* [24].
[b]^{16}N β^- decay P$_\gamma$ from the evaluation of Tilley *et al.* [24].

TABLE V. ^{12}C(n,γ) energies and transition probabilities measured on a graphite powder target.

E_γ	Mult[a]	ICC(ΔICC)	$I_\gamma(\Delta I_\gamma)$	$P_\gamma(\Delta P_\gamma)$
595.16(9)	E1	$3.58(5)\times10^{-6}$	0.0364(15)	0.0248(9)
1261.71(6)	E1	0.000101(2)	47.5(11)	32.1(4)
1856.98(22)	M1	0.000185(3)	0.0238(15)	0.0162(9)
3088.80(21)	E1	0.00128(2)	0.063(3)	0.041(12)
3684.02(7)	M1+E2[b]	0.00091(1)	46.7(11)	32.0(4)
4945.30(7)	E1	0.00201(3)	100.0(19)	67.8(4)

[a]From the evaluation of Ajzenberg-Selove [12].
[b]The mixing ratio $\delta = +0.094(9)$ [12].

TABLE VI. Standardization of the 4945.30-keV γ-ray cross section from the ^{12}C(n,γ) reaction and determination of the total radiative thermal neutron cross section. Here we assume that $P_\gamma(4945) = 67.8 \pm 0.4\%$ from Table VI and the natural abundance of ^{12}C is $98.93 \pm 0.08\%$ [17]. The weighted average includes a statistical uncertainty of 0.03 mb with $\chi^2/f = 0.7$ and a standardization uncertainty of 0.01 mb.

Standard	Formula	Comparator	$\sigma_\gamma(\Delta\sigma_\gamma)$	$\sigma_0(\Delta\sigma_0)$
				(mb)
Polyethylene	$(C_2H_4)_n$	H(2223)	2.67(7)	3.93(10)
Melamine	$C_3H_6N_6$	H(2223)	2.64(4)	3.90(6)
Urea	CH_4N_2O	N(1885)	2.73(10)	4.03(14)
Pyridine	C_5H_5N	H(2223)	2.621(22)	3.87(3)
Pyridine	C_5H_5N	N(1885)	2.604(23)	3.84(3)
		Weighted average		3.87(3)

TABLE VII. Comparison of previous measurements with the new ^{12}C(n,γ) neutron cross section reported here.

σ_0 (mb)	Reference	Method
3.30 ± 0.15	Hennig (1957) [27]	Mass spectroscopy
3.85 ± 0.15	Koechlin (1957) [28]	Pile oscillator
3.5 ± 0.3	Muehlhause (1957) [29]	Pile oscillator
3.80 ± 0.04	Nichols (1960) [30]	Reactivity
3.83 ± 0.06	Starr (1962) [31]	Pulsed neutron
3.8 ± 0.4	Jurney (1963) [20]	PGAA
3.72 ± 0.15	Sagot (1963) [32]	Pulsed neutron
3.50 ± 0.16	Prestwich (1981) [33]	PGAA
3.53 ± 0.07	Jurney (1982) [26]	PGAA
3.53 ± 0.07	Mughabghab (2006) [16]	Compilation
3.87 ± 0.03	This work	PGAA

TABLE VIII. ^{13}C(n,γ) energies and transition probabilities measured on a graphite powder target.

$E_\gamma(\Delta E_\gamma)$	Mult[a]	ICC(ΔICC)	$I_\gamma(\Delta I_\gamma)$	$P_\gamma(\Delta P_\gamma)$
495.71(10)	E1	$5.73(8)\times10^{-6}$	7.5(4)	6.4(3)
808.82(10)	M1	$2.40(4)\times10^{-6}$	5.3(3)	4.45(22)
1273.82(13)	M1	$1.65(2)\times10^{-5}$	5.3(5)	4.45(22)
1586.91(10)	E1	0.00034(1)	8.3(7)	6.5(3)
2082.56(10)	M1	0.00028(1)	5.3(11)	3.3(4)
6092.46(10)	E1	0.00232(4)	15.9(5)	14.2(4)
6587.93(22)	E0		0.1(1)	0.077(9)
8174.04(10)	E1	0.00276(4)	100.0(20)	85.5(5)

[a]From the evaluation of Ajzenberg-Selove [12].

TABLE IX. Standardization of the 6092.46- and 8174.04-keV γ-ray cross sections from the ^{13}C(n,γ) reaction and determination of the total radiative thermal neutron cross section. Here we assume that $P_\gamma(6092) = 14.2 \pm 0.4\%$ and $P_\gamma(8174) = 85.5 \pm 1.7\%$ from Table VIII. The weighted average includes a statistical uncertainty of 0.018 mb with $\chi^2/f = 0.5$ and a standardization uncertainty of 0.003 mb.

Measurement	E_γ	$\sigma_\gamma(\Delta\sigma_\gamma)$	$\sigma_0(\Delta\sigma_0)$
			(mb)
Urea-1	6092	0.207(6)	1.45(4)
	8174	1.300(24)	1.52(3)
Urea-2	6092	0.187(5)	1.32(3)[a]
	8174	1.275(21)	1.491(25)
Urea-3	6092	0.225(16)	1.59(11)
	8174	1.27(4)	1.48(4)
	Weighted average		1.496(18)

[a]Not used in the weighted average.
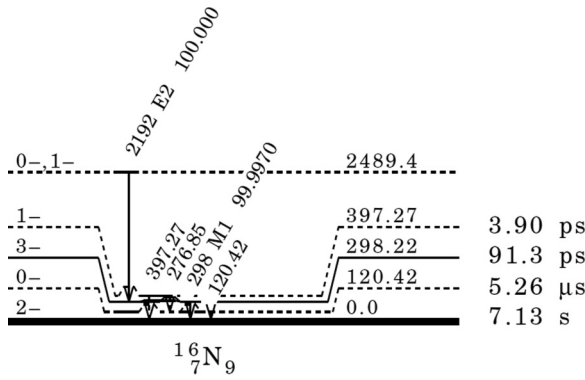
FIG. 2. Decay scheme for ^{15}N(n,γ). The levels at 120.42 and 397.27 keV were not populated in this reaction. Total transition probabilities $P_{\gamma+e}$ are shown.

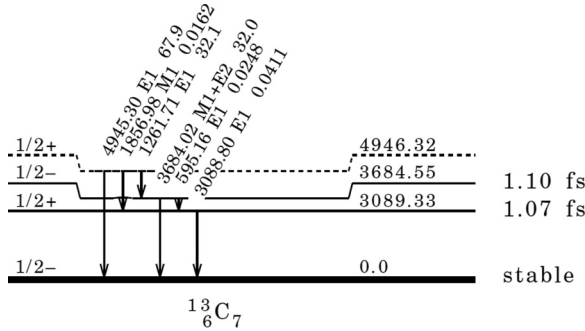FIG. 5. Decay scheme for ^{10}B(n,γ). Total transition probabilities $P_{\gamma+e}$ are shown. The fit of the γ rays to the level scheme gives $\chi^2/f = 2.4$.

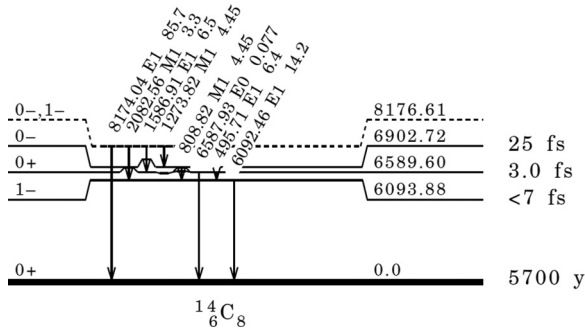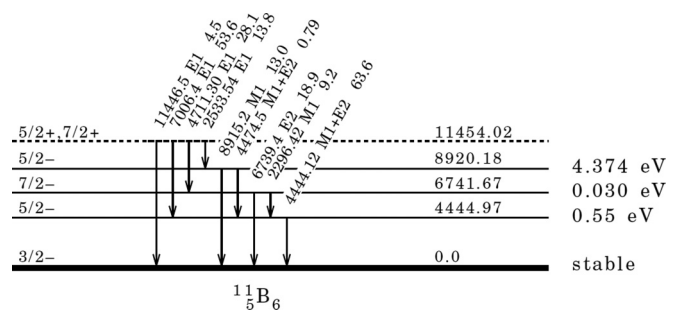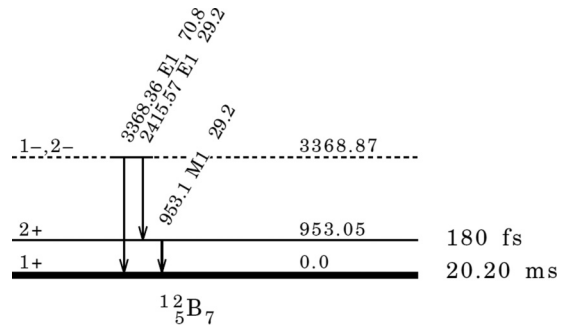FIG. 3. Decay scheme for ^{12}C(n,γ). Total transition probabilities $P_{\gamma+e}$ are shown. The fit of the γ rays to the level scheme gives $\chi^2/f = 0.6$.

FIG. 6. Decay scheme for ^{11}B(n,γ). Total transition probabilities $P_{\gamma+e}$ are shown. The fit of the γ rays to the level scheme gives $\chi^2/f = 0.3$.

FIG. 4. Decay scheme for ^{13}C(n,γ). Total transition probabilities $P_{\gamma+e}$ are shown. The fit of the γ rays to the level scheme gives $\chi^2/f = 0.01$.
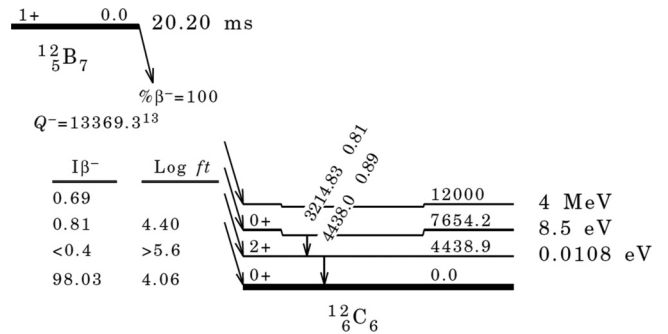
FIG. 7. ^{12}B β^- decay scheme. The level at 12 MeV represents β^- decay feeding to a continuum of levels near that energy. Total transition intensities $P_{\gamma+e}$ are shown.

TABLE X. Previous measurements of the new ^{13}C(n,γ) neutron cross section.

σ_0 (mb)	Reference	Method
0.9 ± 0.2	Hennig (1954) [34]	Activation
1.0 ± 0.3	Bartholomew (1957) [35]	PGAA
0.8 ± 0.2	Bartholomew (1961) [36]	PGAA
1.37 ± 0.04	{Mughabghab (1982) [37]	PGAA
1.502 ± 0.027^{a}		
1.496 ± 0.018	This work	PGAA

[a]Recalculated assuming $\sigma_0(^{12}C) = 3.87 \pm 0.03$ mb, from this work, and $\sigma_0(^{13}C)/\sigma_0(^{12}C) = 0.388 \pm 0.010$ [37].

B. ^{15}N cross section

The ^{15}N(n,γ) thermal neutron radiative neutron capture decay scheme was not previously measured. To determine this cross section we irradiated a 98% ^{15}N enriched pyridine (C$_5$H$_5$N) target with cold neutrons. We identified three γ rays that are assigned to this reaction and listed in Table IV. The 2192-keV γ ray is placed as a primary transition deexciting the CS to the 298.22-keV level [24] which decays by the 298-keV γ ray to the GS. Both transitions have approximately equal intensities so this appears to be a simple γ-ray cascade as shown in Fig. 2. The third transition is the well known 6129-keV γ ray from ^{16}N β^- decay.

The ^{15}N(n,γ) capture state should have $J^\pi = 0^-, 1^-$ assuming s-wave capture. This decay scheme is unusual because the only primary γ ray populates the 298.22 keV 3^- level with an E2 transition, while the expected M1 transitions to levels at $0(2^-)$-, $120.42(0^-)$, and $397.27(1^-)$-keV level are not observed.

The γ-ray cross sections in Table IV were standardized with respect to the 2223-keV γ ray from hydrogen and corrected for abundance in the ^{15}N enriched pyridine sample. Total radiative neutron cross sections were determined for each transition in Table IV leading to a consistent set of values. The weighted average total cross section was determined as $\sigma_0(^{15}N) = 39.6 \pm 1.4$ μb. Here the uncertainty is nearly entirely statistical. This value is larger than the Mughabghab's compiled value $\sigma_0(^{15}N) = 24 \pm 8$ μb [16], although no pri-

FIG. 9. Decay scheme for ^{6}Li(n,γ). Total transition probabilities $P_{\gamma+e}$ are shown. The fit of the γ rays to the level scheme gives $\chi^2/f = 0.07$.

mary reference is given. Another measurement reported by Ferguson and Montague [25] gave $\sigma_0(^{15}N) = 62 \pm 6$ μb, after correction for a more recent ^{37}Cl(n,γ) calibration cross section, is larger than our value but does not appear to have been included in the compilation.

C. ^{12}C cross section

Graphite powder was irradiated for 35 903 s in the cold beam at the Budapest Reactor and six γ rays were assigned to the ^{12}C(n,γ) reaction whose energies and intensities are summarized in Table V. The ^{12}C(n,γ) level scheme drawing is shown in Fig. 3. Transition probabilities were fit to the level scheme with a $\chi^2/f = 0.33$. The neutron separation energy $S_n = 4946.32 \pm 0.06$ keV is in excellent agreement with the recommended value of $S_n = 4946.3084 \pm 0.0005$ keV [10].

The cross section for the 4945.30-keV γ ray was standardized with respect to the 2223-keV γ ray from hydrogen and the 1885-keV γ ray from nitrogen with five stoichiometric compounds as shown in Table VI. We adopt a total cross section $\sigma_0(^{12}C) = 3.87 \pm 0.03$ mb including a statistical uncertainty of 0.03 mb and a standardization uncertainty of 0.01 mb.

There has been considerable variation in the measured ^{12}C(n,γ) cross sections in the past as shown in Table VII. The value $\sigma_0 = 3.53 \pm 0.07$ mb, adopted by Mughabghab [16], was based on the measurement by Jurney *et al.* [26] and is $\approx$9% lower than our value. Since our result is consistent with most other previous measurements and comprised of
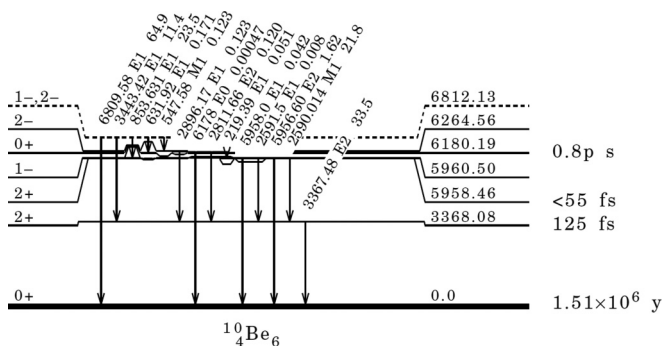

FIG. 8. Decay scheme for ^{9}Be(n,γ). Total transition intensities $P_{\gamma+e}$ are shown. The fit of the γ rays to the level scheme gives $\chi^2/f = 1.0$.
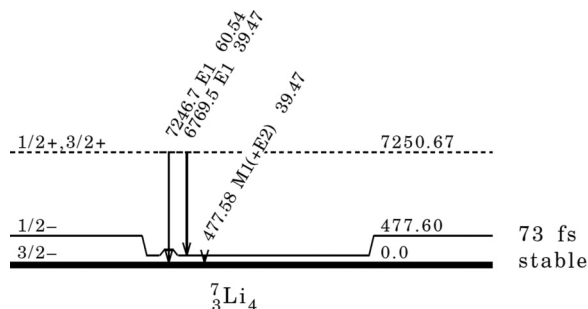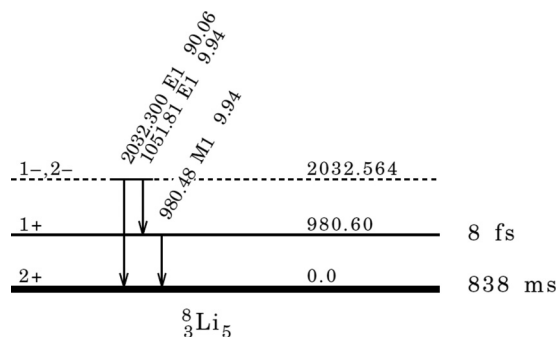

FIG. 10. Decay scheme for ^{7}Li(n,γ). Total transition probabilities $P_{\gamma+e}$ are shown. The fit of the γ rays to the level scheme gives $\chi^2/f = 0.06$.

TABLE XI. ^{10}B(n,γ) energies and transition probabilities were measured on natural H$_3$BO$_3$ and B$_4$N targets. They are compared here with comparable values measured by Kok *et al.* [38] measured on a B$_4$N target with a pair spectrometer.

This work	$E_\gamma(\Delta E)$	Adopted	Mult[a]	MR(δ)	ICC(ΔICC)	H$_3$BO$_3$	$I_\gamma(\Delta I_\gamma)$		Average	$P_\gamma(\Delta P_\gamma)$
	Kok [38]						B$_4$N	Kok [38]		
2296.42(9)	2296.6(6)	2296.42(9)	M1		0.00036(1)	14.4(9)	14(3)	10(6)	14.2(9)	9.2(5)
2533.54(7)	2533.49(23)	2533.54(7)	E1		0.00099(2)	22.3(10)	21(3)	18(6)	22.1(9)	13.8(4)
4444.12(14)	4444.03(12)	4444.07(9)	M1+E2	$+0.158^{25}_{2}$	0.00116(2)	100(3)	100(8)	100(6)	100(3)	63.0(10)
4474.5(3)		4474.5(3)	M1+E2	$+0.061^{25}_{2}$	0.00117(2)	1.1(3)	1.15(18)		1.15(16)	0.79(8)
4711.30(15)	4711.17(10)	4711.21(8)	E1		0.00193(3)	43.7(20)	40(3)	42(3)	42.4(15)	28.0(7)
6739.4(3)	6738.3(5)	6739.11(3)	E2		0.00192(3)	30.3(17)	29(3)	28(3)	29.5(15)	18.9(7)
7006.4(3)	7006.75(10)	7006.72(9)	E1		0.00253(4)	75(4)	84(6)	84(3)	81.0(22)	53.5(10)
8915.2(4)	8916.8(3)	8916.22(24)	M1		0.00277(6)	16.3(13)	19.7(20)	19.4(15)	18.0(9)	13.0(4)
11446.5(13)	11447.4(5)	11447.28(5)	E1		0.00325(6)	5.8(9)	7.2(8)	6.9(4)	6.8(4)	4.44(25)

[a]From the evaluation of Kelley *et al.* [39].

multiple measurements on stoichiometric compounds using several internal standards, we believe that these results should finally settle the previous discrepancies.

D. ^{13}C cross section

We irradiated a urea target (CH$_4$N$_2$O) enriched to 99.5% in ^{13}C and 99.1% in ^{15}N in the cold neutron beam at the Budapest Reactor and seven γ rays were assigned to the ^{12}C(n,γ) reaction whose energies and intensities are summarized in Table VIII and on the level scheme drawing in Fig. 4. The transition probabilities were fit to the level scheme with a $\chi^2/f = 1.1$. An additional weak 6587.93-keV E0 transition was placed in the level scheme based on the evaluation of Ajzenberg-Selove [12]. The neutron separation energy $S_n = 8176.61(8)$ keV is slightly higher than the recommended value $S_n = 8176.43$ keV [10].

The 6092.46- and 8174.04-keV γ-ray cross sections were standardized relative to the 2223-keV γ ray from hydrogen in

TABLE XII. The ^{10}B(n,γ) cross sections determined from a H$_3$BO$_3$ target, relative to hydrogen, and a B$_4$N target, relative to nitrogen. The total radiative cross section $\sigma_0(^{10}$B) is determined from a weighted average of the γ-ray cross sections σ_γ and the transition probabilities in Table XI according to Eq. (1). The weighted average includes a statistical uncertainty of 6 mb with $\chi^2/f = 0.4$, a standardization uncertainty of 0.8 mb, and a 14 mb uncertainty from the ^{10}B abundance.

$E_\gamma(\Delta E_\gamma)$ (keV)	H$_3$BO$_3$ $\sigma_\gamma(\Delta\sigma_\gamma)$ B$_4$N	Wt. Ave.	$\sigma_0(\Delta\sigma_0)$ (mb)
2 296.42(9)	36.5(24) 35(8)	36.4(23)	395(25)
2 533.54(7)	56.5(25) 54(8)	56.3(24)	408(17)
4 444.07(9)	256(8) 255(20)	256(8)	403(12)
4 474.5(3)	2.9(9) 2.9(5)	2.9(4)	372(51)
4 711.21(8)	109(5) 101(8)	106(4)	380(15)
6 739.11(3)	76(5) 74(7)	75(4)	396(22)
7 006.72(9)	207(11) 214(16)	210(9)	392(17)
8 916.22(24)	46(4) 50(5)	47(3)	365(23)
11 447.28(5)	17(3) 18.3(20)	17.9(16)	404(35)
		Weighted average	394(15)

the urea sample as summarized in Table IX. Three separate measurements were made that give a weighted average cross section $\sigma_0(^{13}$C$) = 1.496 \pm 0.018$ mb. The uncertainty consists of a statistical contribution of 0.018 mb and a standardization contribution of 0.003 mb.

Our result is compared with previous measurements in Table X. The only previous precise measurement was by Mughabghab *et al.* [37] and is $\approx$9% lower than our result. They measured $\sigma_0(^{13}$C$)/\sigma_0(^{12}$C$) = 0.388 \pm 0.010$ which, when combined with our new ^{12}C cross section, gives $\sigma_0(^{13}$C$) = 1.502 \pm 0.027$ mb in excellent agreement with our $\sigma_0(^{13}$C$)$ measurement.

E. ^{10}B cross section

The ^{10}B transition γ-ray cross sections were measured on H$_3$BO$_3$ and B$_4$N targets and standardized with respect to the hydrogen and nitrogen γ-ray cross sections, respectively. This standardization was done assuming the natural abundance of ^{10}B is 19.9 ± 0.7%. The hydrogen stoichiometry was corrected for an 0.5% background from water in the sample based on the relative intensity of the 2223-keV hydrogen γ ray with respect to the intense 478-keV γ ray from the ^{10}B(n,α) reaction assuming $\sigma_\gamma(478) = 719 \pm 5$ b [16,40].

The ^{10}B(n,γ) transition energies and intensities are summarized in Table XI and the ^{11}B decay scheme is shown in Fig. 5. The transition probabilities were fit to the level scheme with a $\chi^2/f = 1.4$. In Table XI we have averaged our transition

TABLE XIII. ^{11}B(n,γ) energies and transition probabilities were measured on a natural H$_3$BO$_3$ target. The weighted average includes a statistical uncertainty of 0.06 mb with $\chi^2/f = 0.02$, a standardization uncertainty of 0.02 mb, and an uncertainty from the ^{11}B abundance of 0.08 mb.

$E_\gamma(\Delta E_\gamma)$	$\sigma_\gamma(\Delta\sigma_\gamma)$	Mult[a]	ICC(ΔICC)	$P_\gamma(\Delta P_\gamma)$	$\sigma_0(\Delta\sigma_0)$
953.1(6)	2.66(19)	M1	1.00×10^{-6}	29.2(5)	9.11(16)
2415.57(12)	2.65(8)	E1	0.00092(2)	29.2(5)	9.06(16)
3368.36(17)	6.43(8)	E1	0.00142(2)	70.7(5)	9.09(6)
				Weighted average	9.09(10)

[a]From the evaluation of Ajzenberg-Selove [42].

TABLE XIV. Energies and transition probabilities measured on a beryllium metal target and cross sections measured with a natural Be(NO$_3$)$_2$ target. The weighted average includes a statistical uncertainty of 0.12 mb with $\chi^2/f = 0.1$ and a standardization uncertainty of 0.03 mb.

$E_\gamma(\Delta E_\gamma)$	Mult[a]	ICC(ΔICC)	$I_\gamma(\Delta I_\gamma)$	$P_\gamma(\Delta P\sigma_\gamma)$	$\sigma_\gamma(\Delta\sigma_\gamma)$	$\sigma_0(\Delta\sigma_0)$
219.39(13)	E1		0.078(10)	0.051(4)		
547.58(4)	M1		0.188(17)	0.123(9)		
631.92(4)	E1		0.31(7)	0.171(14)		
853.631(11)	E1		36.1(9)	23.5(5)	1.92(5)	8.16(26)
2590.014(25)[b]	M1	0.00049(1)	33.7(8)	21.8(5)	1.82(11)	8.4(6)
2591.5(6)[c]	E1	0.00103(2)	0.013(6)	0.008(4)		
2811.66(16)	E2	0.00070(1)	0.181(21)	0.120(13)		
2896.17(11)	E1	0.00119(2)	0.200(22)	0.123(9)		
3367.48(4)	E2	0.00094(1)	52.6(12)	33.5(5)	2.81(7)	8.40(23)
3443.42(4)	E1	0.00140(2)	17.5(6)	11.4(4)	0.94(4)	8.3(4)
5956.60(9)	E2	0.00175(3)	2.52(21)	1.62(13)		
5958.0(6)[c]	E1	0.00229(4)	0.065(7)	0.042(4)		
6180.19(5)	E0		0.00047(16)	0.0003(1)		
6809.58(10)	E1	0.00249(4)	100.0(24)	64.7(5)	5.31(13)	8.21(21)
				Weighted average		8.27(13)

[a]From the evaluation of Tilley *et al.* [43].
[b]Transition intensity corrected for background interference.
[c]Expected transition taken from Tilley *et al.* [43] and normalized to level feeding intensity.

energies and intensities with the previously published data of Kok *et al.* [38]. The neutron separation energy determined in our work, $S_n = 11\,454.02 \pm 0.10$ keV, is in excellent agreement with the adopted value, $S_n = 11\,454.12 \pm 0.16$ keV [10].

The γ-ray cross sections were determined for all transitions in our work relative to hydrogen and nitrogen and are summarized in Table XII. We determined the total cross sections $\sigma_0(^{10}\text{B})$ from the weighted average γ-ray cross sections and transition probabilities according to Eq. (1). Agreement between the two calibrations was good and we get a weighted average cross section $\sigma_0(^{11}\text{B}) = 394 \pm 15$ mb. The error is comprised of 6 mb statistical uncertainty, 0.8 mb calibration uncertainty, and 14 mb uncertainty in the abundance of ^{10}B. This result agrees with the earlier measurement by Bartholomew and Campion [19] (500 ± 200 mb) but is higher than the value determined by Kok *et al.* [38] (290 ± 40 mb) and the recommended value of Mughabghab [16] (305 ± 16 mb).

TABLE XV. Comparison of the previous measurements of the $^9\text{Be}(n,\gamma)$ total radiative thermal neutron cross sections with the new measurements reported here.

σ_0 (mb)	Reference	Method
10.2 ± 0.5	Nobles (1947) [45]	Diffusion length
9 ± 3	Hughes (1947) [46]	Activation
8.5 ± 0.3	Anderson (1947) [47]	Pile oscillator
7.5 ± 1.0	Jarcyzk (1961) [48]	PGAA
9.3 ± 1.6	Vidal (1963) [49]	Pile oscillator
8.49 ± 0.34	Conneely (1986) [50]	PGAA
8.49 ± 0.34	Mughabghab (2006) [16]	Compilation
8.27 ± 0.13	This work	PGAA

F. ^{11}B cross section

^{12}B transition probabilities and cross sections from $^{11}\text{B}(n,\gamma)$ are summarized in Table XIII and the ^{12}B decay scheme is shown in Fig. 6. Transition probabilities were fit to the level scheme with a $\chi^2/f = 0.01$.

The neutron separation energy was determined as 3368.87 ± 0.16 keV, which is consistent with the recommended value of 3369.8 ± 1.4 keV [10]. The total thermal radiative neutron cross section was determined with respect to the 2223-keV γ ray from hydrogen as $\sigma_0 = 9.09 \pm 0.10$ mb including a statistical uncertainty 0.06 mb, a standardization uncertainty of 0.02 mb, and an uncertainty from the abundance of 0.08 mb. This result is consistent with and more precise than the only other measurement $\sigma_0 = 5 \pm 3$ mb, by Imhof *et al.* [41], and the recommended value $\sigma_0 = 5.5 \pm 3.3$ mb, by Mughabghab [16].

^{12}B also β^- decays with a half-life of 20.20 ± 0.02 ms [43]. Two γ rays were observed from this decay at 3214.8 keV, with $\sigma_\gamma = 74 \pm 16$ μb, and 4438.0 keV, with $\sigma_\gamma = 81 \pm 18$ μb. The β-decay transition probabilities can be calculated from the ratios of their cross sections to the total radiative neutron cross section σ_0, leading to the ^{12}B β^- decay scheme shown in Fig. 7. The β-decay feeding to the 7654.2 keV level is $0.81 \pm 0.18\%$, which is slightly larger than the value $0.58 \pm 0.02\%$ measured by Hildegaard *et al.* [44] but lower than the evaluated value by Tilley *et al.* of $1.5 \pm 0.3\%$ [43]. We set an upper limit of 0.4% feeding to the 4438.9 keV state which is consistent with no feeding found by Hildegaard *et al.*, but it is inconsistent with $1.2 \pm 0.3\%$ adopted by Tilley *et al.*

G. ^9Be cross section

The $^9\text{Be}(n,\gamma)$ transition probabilities and cross sections were measured on a block of pure beryllium and are sum-

TABLE XVI. ^{6,7}Li(n,γ) energies, intensities, and γ-ray cross sections measured on a LiF target enriched to 98% in ^{7}Li and a natural Li$_2$CO$_3$ target. Three separate measurements were performed on the Li$_2$CO$_3$ target.

Reaction	$E_\gamma(\Delta E_\gamma)$	Mult[a]	ICC(ΔICC)	^{7}LiF $I_\gamma(\Delta I_\gamma)$	^{nat}Li$_2$CO$_3$ $I_\gamma(\Delta I_\gamma)$-1	$I_\gamma(\Delta I_\gamma)$-2	$I_\gamma(\Delta I_\gamma)$-3	Weighted average	$P_\gamma(\Delta P_\gamma)$
^{6}Li(n,γ)	477.58(4)	M1			65.9(26)	67.8(22)	65.2(9)	65.6(8)	39.47(16)
	6769.5(3)	E1	0.00248(4)		65.1(17)	65.1(11)	65.3(5)	65.2(4)	39.37(20)
	7246.7(3)	E1	0.00258(4)		100.0(24)	100.0(17)	100.0(15)	100.0(10)	60.38(18)
	$\sigma_\gamma(7247)$				24.2(6)	24.0(7)	23.3(5)	23.7(3)	$\sigma_0 = 39.3(7)$ mb[b]
^{7}Li(n,γ)	980.60(7)	M1		10.80(18)	11.3(3)	11.1(3)	11.01(21)	11.00(11)	9.94(6)
	1051.81(5)	E1		10.77(19)	11.6(3)	11.1(3)	11.13(23)	11.07(12)	9.94(6)
	2032.300(20)	E1	0.00067(1)	100.00(16)	100.0(19)	100.0(22)	100.0(17)	100.00(16)	90.00(5)
	$\sigma_\gamma(2032)$			39.5(8)	39.4(6)	40.5(6)	39.9(6)	39.8(3)	$\sigma_0 = 44.3(5)$ mb[c]

[a]From the evaluation of Tilley *et al* [43,51].
[b]The weighted average includes a statistical uncertainty of 0.6 mb with $\chi^2/f = 0.5$, a standardization uncertainty of 0.2 mb, and a 0.2 mb uncertainty from the ^{6}Li abundance.
[c]The weighted average includes a statistical uncertainty of 0.4 mb with $\chi^2/f = 0.5$, a standardization uncertainty of 0.3 mb, and a 0.02 mb uncertainty from the ^{6}Li abundance.

marized in Table XIV and the ^{10}Be thermal neutron decay scheme is shown in Fig. 8. Transition probabilities were fit to the decay scheme with a $\chi^2/f = 0.16$. The ^{10}Be neutron separation energy measure was determined as 6812.13 ± 0.04 keV, which is slightly lower than the recommended value [10] of 6812.28 ± 0.05 keV.

The γ-ray cross sections were measured with a natural Be(NO$_3$)$_2$ target and standardized with respect to nitrogen. Five ^{10}Be γ-ray cross sections that were measured with high precision in this work are summarized in Table XIV. Total thermal radiative neutron cross sections were determined from each of these transitions giving a weighted average cross section $\sigma_0(^9$Be$) = 8.27 \pm 0.13$ mb. The error consists of 0.12 mb statistical uncertainty and 0.03 mb calibration uncertainty. This value is consistent with previous measurements and the adopted value from Mughabghab [16] that are summarized in Table XV.

H. ^{6,7}Li cross sections

The ^{6,7}Li cross sections were measured with a ^{7}LiF target enriched to 98% in ^{7}Li and a natural Li$_2$CO$_3$ target. The γ-ray energies, intensities, and transition probabilities for both reactions are summarized in Table XVI and in the decay scheme drawings in Figs. 9 and 10. Transition probabilities were fit to the level scheme with a $\chi^2/f = 0.08$ for ^{6}Li(n,γ) and $\chi^2/f = 0.23$ for ^{7}Li(n,γ).

The neutron separation energy for ^{7}Li was determined as 7250.67 ± 0.21 keV, slightly lower than the recommended value [10] of $S_n = 7251.09 \pm 0.01$ keV, and the neutron separation energy for ^{8}Li was determined as 2032.564 ± 0.019 keV, consistent with the recommended value of 2032.52 ± 0.05 keV. The cross sections were standardized with respect to the 1633-keV γ ray from ^{20}F decay in the ^{7}LiF target, assuming a cross section of 9.32 ± 0.22 mb [58], and the 4945-keV γ ray in the Li$_2$CO$_3$ target. The γ-ray transition probabilities and cross sections measured in these experiments are summarized in Table XVI. For ^{6}Li we obtained $\sigma_0 = 39.3 \pm 0.7$ mb with a statistical uncertainty of 0.6 mb, a standardization uncertainty of 0.2 mb, and an uncertainty in the abundance of 0.2 mb. For

TABLE XVII. Comparison of the previous measurements of the ^{6,7}Li(n,γ) total radiative thermal neutron cross sections with the new measurements reported here.

Isotope	σ_0 (mb)	Reference	Method
^{6}Li	30 ± 8	Bartholomew (1957) [19]	PGAA
	48 ± 15	Jarcyzk (1961) [48]	PGAA
	38.5 ± 3.0	Jurney (1973) [52]	PGAA
	37.7 ± 3.0	Park (2006) [53]	PGAA
	38.5 ± 3.0	Mughabghab (2006) [16]	Compilation
	39.3 ± 0.7	This work	PGAA
^{7}Li	33 ± 5	Hughes (1947) [54]	Activation
	42 ± 10	Kotypin (1956) [55]	Activation
	40 ± 8	Imhof (1959) [56]	Activation
	40 ± 12	Jarcyzk (1961) [48]	PGAA
	45.4 ± 3.0	Lynn (1991) [57]	PGAA
	45.5 ± 2.7	Mughabghab (2006) [16]	Compilation
	44.3 ± 0.5	This work	PGAA

TABLE XVIII. Total thermal radiative neutron cross sections measured in this work.

Reaction	σ_0 (mb) This work	Atlas [16]
^{6}Li(n,γ)	39.3(7)	38.5(30)
^{7}Li(n,γ)	44.3(5)	45.4(27)
^{9}Be(n,γ)	8.27(13)	8.49(34)
^{10}B(n,γ)	394(15)	305(16)
^{11}B(n,γ)	9.09(10)	5.5(33)
^{12}C(n,γ)	3.87(3)	3.53(7)
^{13}C(n,γ)	1.496(18)	1.37(4)
^{14}N(n,γ)	80.0(4)	80.1(6)
^{15}N(n,γ)	39.6(14)[a]	24(8)[a]

[a]Cross section in μb.

^{7}Li we obtained $\sigma_0 = 44.3 \pm 0.5$ mb with an 0.4 mb statistical uncertainty, 0.3 mb standardization uncertainty, and 0.02 mb uncertainty in the abundance. These values are consistent with previous measurements summarized in Table XVII.

V. DISCUSSION

The γ-ray energies, transition probabilities, neutron separation energies, and total thermal radiative neutron cross sections for the isotopic targets ^{6,7}Li, ^{9}Be, ^{10,11}B, ^{12,13}C, and ^{14,15}N have been measured in this work, These cross sections, summarized in Table XVIII, are the result of multiple measurements with multiple standards. They are generally more precise and frequently in significant disagreement with the earlier recommended values of Mughabghab [16]. We have established a new method of determining transition probabilities that incorporate the constraints of the level scheme for these complete capture γ-ray measurements.

[1] T. Belgya, Z. Revay, I. H. B. Fazekas, L. Dabolczi, G. L. Molnár, J. O. Z. Kis, and G. Kaszás, *Proceedings of the 9th International Symposium on Capture Gamma-Ray Spectroscopy and Related Topics*, edited by G. Molnár, T. Belgya, and Zs. Révay (Springer, Berlin, 1997), p. 826.

[2] Z. Revay, T. Belgya, Z. Kasztovszky, J. L. Weil, and G. A. Molnár, Nucl. Instrum. Meth. B **213**, 385 (2004).

[3] R. B. Firestone, H. D. Choi, R. M. Lindstrom, G. L. Molnár, S. F. Mughabghab, R. Paviotti-Corcuera, Z. Revay, V. Zerkin, and C. M. Zhou, *Database of Prompt Gamma Rays from Slow Neutron Capture for Elemental Analysis* (IAEA STI/PUB/1263, 251, 2007).

[4] G. L. Molnár, Ed., *Handbook of Prompt Gamma Activations Analysis with Neutron Beams* (Kluwer Academic, Boston, 2004).

[5] *Strategic and Critical Materials 2013 Report on Stockpile Requirements* (Office of the Under Secretary of Defense for Acquisition, Technology and Logistics, Department of Defense, 2013).

[6] R. B. Firestone and Zs. Revay, Phys. Rev. C **93**, 044311 (2016).

[7] G. L. Molnár, Z. Revay, and T. Belgya, Nucl. Instrum. Meth. Phys. Res. A **489**, 140 (2002).

[8] B. Fazekas, J. Óstór, Z. Kis, G. L. Molnár, and A. Simonits, *Proceedings of the 9th International Symposium on Capture Gamma-Ray Spectroscopy and Related Topics*, edited by G. Molnár, T. Belgya, and Zs. Révay (Springer, Berlin, 1997), p. 774.

[9] R. B. Firestone, Lawrence Berkeley Laboratory Report LBL-26024 (1994).

[10] M. Wang, G. Audi, A. H. Wapstra, F. G. Kondev, M. MacCormick, X. Xu, and B. Pfeiffer, Chin. Phys. C **36**, 1603 (2012).

[11] T. Belgya, Phys. Rev. C **74**, 024603 (2006).

[12] F. Ajzenberg-Selove, Nucl. Phys. A **523**, 1 (1991).

[13] E. T. Jurney, J. W. Starner, J. E. Lynn, and S. Raman, Phys. Rev. C **56**, 118 (1997).

[14] T. Kibedi, T. W. Burrows, M. B. Trzhaskovskaya, P. M. Davidson, and J. C. W. Nestor, Nucl. Instrum. Meth. A **589**, 202 (2008).

[15] Evaluated Nuclear Structure Data File (ENSDF) maintained at the National Nuclear Data Center, Brookhaven National Laboratory, Upton, NY.

[16] S. F. Mughabghab, *Atlas of Neutron Resonances*, 5th ed. (Elsevier, New York, 2006).

[17] M. Berglund and M. E. Wieser, Pure Appl. Chem. **83**, 397 (2011).

[18] B. B. Kinsey, G. A. Bartholomew, and W. H. Walker, Can. J. Phys. **29**, 1 (1951).

[19] G. A. Bartholomew and P. J. Campion, Can. J. Phys. **35**, 1347 (1957).

[20] E. Jurney and H. Motz, Argonne National Laboratory report series No. 6797, p. 236 (1963).

[21] M. A. Islam, W. V. Prestwich, and T. J. Kennett, Nucl. Instrum. Meth. **188**, 243 (1981).

[22] M. A. Islam, T. J. Kennett, and W. V. Prestwich, Nucl. Instrum. Meth. **287**, 460 (1990).

[23] Y. E. Loginov, L. M. Smotritskiy, and P. Sushlov, Nucl. Instrum. Meth. A **545**, 296 (2005).

[24] D. R. Tilley, H. R. Weller, and C. M. Cheves, Nucl. Phys. A **564**, 1 (1993).

[25] A. J. Ferguson and J. H. Montague, Phys. Rev. **87**, 215 (1952).

[26] E. T. Jurney, P. J. Bendt, and J. C. Browne, Phys. Rev. C **25**, 2810 (1982).

[27] G. R. Hennig, *The slow neutron absorption cross section of graphite*, Brookhaven National Laboratory Report BNL-489, 19 (1957).

[28] J. C. Koechlin, P. Tanguy, and C. P. Zeleski, *French results on natural uranium-graphite lattices*, Brookhaven National Laboratory Report BNL-489, 97 (1957).

[29] C. O. Muehlhause, S. P. Harris, D. Rose, H. P. Schroeder, G. E. Thomas, and S. Wexler, *The slow neutron absorption cross section of graphite*, Brookhaven National Laboratory Report BNL-489, 21 (1957).

[30] P. F. Nichols, Nucl. Sci. Eng. **7**, 395 (1960).

[31] E. Starr and G. A. Price, Proc. Brookhaven Conf. Neutron Thermalization BNL-719, 1034 (1962).

[32] M. Sagot and H. Tellier, J. Nucl. Energy Parts A/B **17**, 347 (1963).

[33] W. V. Prestwich, M. A. Islam, and T. J. Kennett, Nucl. Sci. Eng. **78**, 182 (1981).

[34] R. H. G, Phys. Rev. **95**, 92 (1954).

[35] G. A. Bartholomew, J. W. Knowles, G. Manning, and P. J. Campion, *Pair spectrometer and flat crystal spectrometer*, Atomic Energy Canada Ltd. AECL Report No. 36, 36 (1957).

[36] G. A. Bartholomew, Ann. Rev. Nucl. Sci. **11**, 259 (1961).

[37] S. F. Mughabghab, M. A. Lone, and B. C. Robertson, Phys. Rev. C **26**, 2698 (1982).

[38] P. J. J. Kok, J. B. M. de Haas, K. Abrahams, H. Postma, and W. J. Huiskamp, Z. Phys. A-Atomic Nuclei **324**, 271 (1986).

[39] J. H. Kelley, E. Kwan, J. E. Purcell, C. G. Sheu, and H. R. Weller, Nucl. Phys. A **880**, 88 (2012).

[40] A. Gopfert, F. J. Hambsch, and H. Bax, Nucl. Instrum. Meth. Phys. Res. A **441**, 438 (2000).

[41] W. L. Imhof, R. G. Johnson, F. J. Vaughn, and M. Walt, Phys. Rev. **125**, 1334 (1962).

[42] F. Ajzenberg-Selove, Nucl. Phys. A **506**, 1 (1990).

[43] D. R. Tilley, J. H. Kelley, J. L. Godwin, D. J. Millener, J. E. Purcell, C. G. Sheu, and H. R. Weller, Nucl. Phys. A **745**, 155 (2004).

[44] S. Hyldegaard, C. Forssen, C. A. Diget, M. Alcorta, and F. C. Barker, Phys. Lett. B. **678**, 459 (2009).

[45] R. Nobles and J. Wallace, Argonne National Laboratory report series No. 4076, p. 10 (1947).

[46] D. J. Hughes, C. Eggler, and C. M. Huddleston, Phys. Rev. **71**, 269 (1947).

[47] H. L. Anderson, E. Fermi, A. Wattenberg, G. L. Weil, and H. Zinn, Phys. Rev. **72**, 16 (1947).

[48] L. von Jarcyzk, J. Lang, R. Muller, and W. Wolfli, Helv. Phys. Acta **34**, 483 (1961).

[49] R. Vidal, *Oscillator measurements*, Progress report from EURATOM and member countries to the European-American Nuclear Data Committee EANDC(E)-049, 94 (1963).

[50] C. M. Conneely, W. V. Prestwich, and T. J. Kennett, Nucl. Instrum. Meth. Phys. Res. A **248**, 416 (1986).

[51] D. R. Tilley, C. M. Cheves, J. L. Godwin, G. M. Hale, H. M. Hofmann, J. H. Kelley, C. G. Sheua, and H. R. Weller, Nucl. Phys. A **708**, 3 (2002).

[52] E. T. Jurney, U.S. Nuclear Data Commission Report USNDC-109 (1973).

[53] C. S. Park, G. M. Sun, and H. D. Choi, Nucl. Instrum. Meth. Phys. Res. B **245**, 367 (2006).

[54] D. J. Hughes, D. Hall, C. Eggler, and E. Goldfarb, Phys. Rev. **72**, 646 (1947).

[55] E. A. Koltypin and V. M. Morozov, Sov. Phys. Dokl. **1**, 655 (1956).

[56] W. L. Imhof, R. G. Johnson, F. J. Vaughn, and M. Walt, Phys. Rev. **114**, 1037 (1959).

[57] J. E. Lynn, E. T. Jurney, and S. Raman, Phys. Rev. C **44**, 764 (1991).

[58] L. Szentmiklosi, Z. Revay, and T. Belgya, Nucl. Instrum. Meth. Phys. Res. A **564**, 655 (2006).